Modeling of soil water and nitrogen transport characteristics of the furrow irrigation for urea fertilizer using HYDRUS

Zhengjiang Feng, Weibo Nie*, Yunpeng Ma

(*State Key Lab. of Eco-hydraulics in Northwest Arid Region, Xi'an University of Technology, Xi'an 710048, China*)

Abstract: Furrow irrigation is widely used in agriculture practice but faces challenges in inefficient water and nitrogen management, which may contribute to groundwater contamination risks due to nitrate leaching. In this study, soil hydraulic and solute reaction parameters were inversed through HYDRUS-1D and genetic algorithm based on one-dimensional urea solution infiltration experiments to explore the effects of urea concentration (*C*), water depth (WD), furrow bottom width (FW), and soil initial water content (IWC) on soil water and nitrogen transport characteristics of furrow irrigation using HYDRUS-2D simulation. Moreover, structural equation modeling (SEM) quantitatively analyzed these factors. The results showed that the inversed parameters were reliable. The infiltration rate increased with *C*, WD, and FW but decreased with IWC. The urea was completely hydrolyzed on the fifth day of the redistribution process. The ammonium nitrogen (NH_4^+-N) initially increased to the maximum value on the third day and then decreased. The SEM revealed that the IWC, FW, and WD positively affected the aspect ratio of the wetting pattern. It is suggested that WD and FW should be appropriately increased during furrow irrigation. Moreover, to reduce the risk of deep leaching of NO_3^--N, fertigation should be avoided when the soil water content is high in the range of suitable water contents for crop growth. The results provide theoretical insights for improving nitrogen efficiency and supporting sustainable agricultural practices.

Keywords: urea concentration, furrow irrigation, HYDRUS, NO_3^--N leaching

DOI: 10.25165/j.ijabe.20251802.8850

Citation: Feng Z J, Nie W B, Ma Y P. Modeling of soil water and nitrogen transport characteristics of the furrow irrigation for urea fertilizer using HYDRUS. Int J Agric & Biol Eng, 2025; 18(2): 169–178.

1 Introduction

Furrow irrigation is one of the most used methods in agriculture practice owing to its advantage of initial cost, culture, and energy requirements[1]. Furrow fertigation with nitrogen provides an effective and uniform method for distributing water and fertilizer (nutrients) to crops, which has the potential to improve seasonal fertilizer application efficiency compared with traditional broadcast fertilizer application methods[2]. However, less-than-optimum management of furrow systems may cause inefficient water and nutrient utilization, thereby potentially reducing yield benefits and contributing to groundwater pollution through deep water drainage and nitrogen leaching[3,4].

The transfer of water and fertilizer and the reaction of nitrogen are usually affected by several factors, including soil texture, soil initial water content (IWC), fertilizer concentration, enzymatic activity, and soil environmental conditions such as temperature[4–6]. Nitrogen undergoes various transformations, including mineralization, nitrification, denitrification, volatilization, adsorption, and ionic exchange in soils[3,7]. In addition, the transfer and distribution of soil water and fertilizer in furrow irrigation are influenced by other factors, such as furrow bottom width (FW) and water depth (WD)[8]. All these factors make the prediction of soil water and nitrogen more complex, thus making the optimum management of furrow irrigation systems challenging. Conducting experiments to explore all different scenarios of furrow irrigation is costly and time-consuming. In addition, the experiment method has limitations in the optimum management of furrow irrigation[3,9]. The HYDRUS is flexible to adapt to different types of water flow and boundary conditions of solute transport calculation. Additionally, it can simultaneously consider soil water and solute dynamics under different management practices[3,10]. Moreover, HYDRUS-2D has been extensively and successfully used to simulate water and nutrient transport in soils, even for complicated problems under furrow irrigation[11]. The various reaction processes of nitrogen in soils are always predicted using first-order reaction kinetics through the rate constant. However, the reaction processes are complex because of their coupled nature and their sensitivity to soil conditions, such as soil texture, water, and temperature[7,12]. In addition, to ensure the accuracy and reliability of the simulation results, the reasonable soil hydraulic and solute reaction parameters must be determined before conducting the HYDRUS simulation[13].

Urea as organic nitrogen is used extensively in agricultural production and is characterized by stable properties, high nitrogen content, and high solubility, making it a suitable essential nutrient source for crops through fertilization[5,6]. The main decay chain for urea in soil involves the transformation of urea into ammonium (NH_4^+-N) and nitrate nitrogen (NO_3^--N)[7,12]. Nitrogen species, such as NO_3^--N, cannot be adsorbed by soil and are easily transported by water flow, thus resulting in nitrogen leaching. NH_4^+-N is a volatile species that is easily lost through volatilization. Consequently, the decay process of urea is complicated. If the process is not properly managed, it will lead to the loss of nitrogen (urea, NH_4^+-N, and NO_3^--N), low nitrogen utilization efficiency, and environmental pollution, thus posing a threat to human health[14]. Numerous studies have examined the urea decay and transfer process through

Received date: 2024-02-03 **Accepted date:** 2025-03-11

Biographies: ZhengJiang Feng, PhD candidate, research interest: water-saving irrigation theory and technology. Email: fzj13120230@163.com; **YunPeng Ma**, MS, research interest: water-saving irrigation theory and technology. Email: 15036988087@163.com

***Corresponding author: WeiBo Nie**, PhD, Professor, research interest: water-saving irrigation theory and technology. Xi'an University of Technology, Xi'an 710048, China. Tel: +86-13519176470, Email: nwbo2000@163.com.

experiment[12,15] and numerical simulation[16,17]. However, only a few studies have investigated the effects of various factors (such as soil IWC, furrow water depth and bottom width, and concentration of urea solution) on the soil water and nitrogen transport characteristics of furrow fertigation and quantified these effects using structural equation models.

Therefore, this study aimed to 1) inverse the soil hydraulic and solute reaction parameters and verify them; 2) simulate the infiltration and distribution process of urea solution in furrow irrigation under different factors (urea concentration, WD, FW, and IWC) using HYDRUS-2D; 3) use structural equation models to quantitatively analyze the effects of different factors on the infiltration and distribution process of urea solution in furrow irrigation.

2 Materials and methods

2.1 Experimental location and materials

This experiment was conducted from June to August 2022 in Yangling District, Shaanxi Province, in northwestern China (34°17′N, 108°04′E). The climate of the study site was semiarid and semihumid. In addition, the average daytime temperature between June and August was 28.5°C. The soils utilized in this study were classified as sandy loam and clay loam (International reclassification standard), and were collected from a depth range of 0 to 60 cm. The soil was air-dried and sieved to ≤2 mm and the residual water content (θ_r) was measured using the oven-drying method. The field capacities (FCs) were measured using the cutting ring method. The Mastersizer 2000 analyzer (Malvern Panalytical Company) was used to determine the soil particle size. The urea nitrogen in the soil was determined by the diacetyl monoxime colorimetric method using an ultraviolet spectrophotometer (Shimadzu Corporation, Beijing, China)[18]. Nitrate nitrogen (NO_3^--N) and ammonium nitrogen (NH_4^+-N) were measured using an automatic intermittent chemical analyzer (SMARTCHEM 450) (LICA United Technology Limited, Beijing, China). The characteristic parameters of the test soil are listed in Table 1.

Table 1 Characteristic parameters of the test soil

Soil texture	θ_r/cm³·cm⁻³	FC/cm³·cm⁻³	NO_3^--N/mg·kg⁻¹	NH_4^+-N/mg·kg⁻¹	Urea/mg·kg⁻¹	Content of soil particles/%		
						Clay (<0.002 mm)	Silt (0.002–0.020 mm)	Sand (0.020–2.000 mm)
Clay loam	0.035	0.32	6.98	4.53	0.55	28.74	33.46	37.80
Sandy loam	0.023	0.22	4.78	6.01	0.16	15.33	24.89	59.78

Note: θ_r is the residual water content; FC is the field capacity; NO_3^--N and NH_4^+-N are the nitrate nitrogen and ammonium nitrogen, respectively.

2.2 Experiment design

In this study, urea solution was used to conduct one-dimensional (1D) and two-dimensional (2D) infiltration experiments. According to the irrigation practices of local farmers, the infiltration process was terminated when the cumulative infiltration was 80 mm (unit area). The bulk densities of the sandy and clay loam soils were designed to be 1.45 and 1.35 g/cm³, respectively[19]. Seven different concentrations of urea solution (0.2, 0.4, 0.6, 0.8, 1, 3, and 5 g/L) were administered for the 1D vertical infiltration experiment[6,20], and were denoted as T1, T2, T3, T4, T5, T6, and T7, respectively. In addition, a control treatment (0 g/L) was used, denoted as CK. Moreover, five concentrations of urea solution (0.4, 0.8, 1, 3, and 5 g/L) and control treatment (0 g/L) were administered for the 2D furrow infiltration experiment.

For the 1D vertical infiltration experiments, the soil IWC was controlled as θ_r for clay loam and sandy loam (Table 1), respectively. The soil samples were taken from the wetted soil volume at the moments of infiltration termination and the 1st, 3rd, 5th, and 10th days after infiltration to determine the soil water content and the content of urea, NO_3^--N, and NH_4^+-N (Figure 1). The detailed description of the 1D vertical infiltration experiments can be found in Feng et al.[5]. A polymethyl methacrylate soil box was used to conduct the furrow irrigation experiments (Figure 1b), and the IWC was controlled as θ_r for clay loam and sandy loam (Table 1), respectively. The soil samples were collected from different locations at infiltration termination and the 1st, 3rd, 5th, and 10th days after infiltration to determine the soil moisture content and the content of urea, NO_3^--N, and NH_4^+-N.

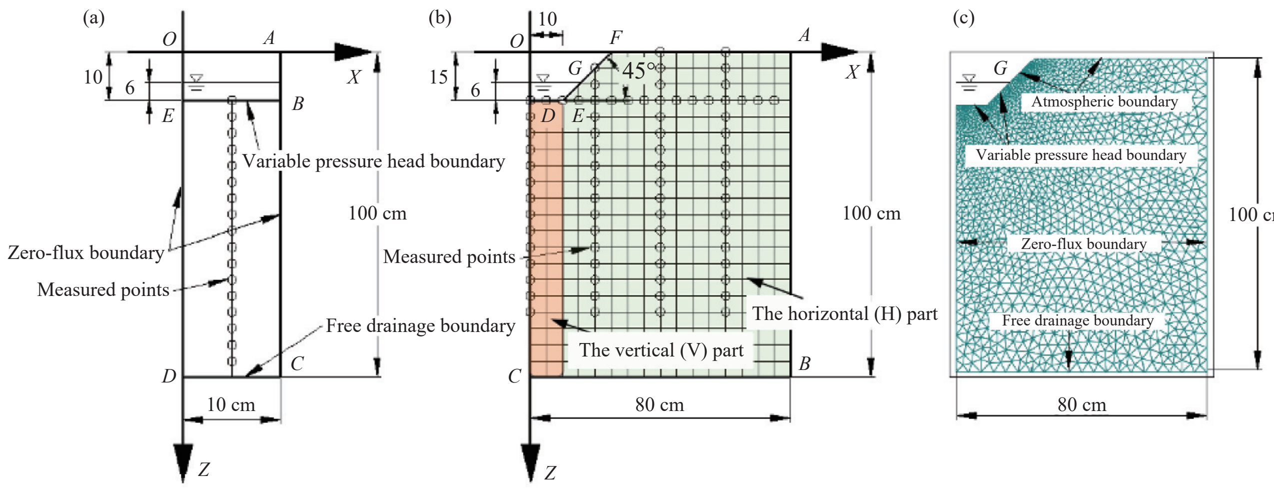

Note: (a) Cross-section, measured points, and boundary condition of soil column; (b) Cross-section and measured points of soil box and furrow; (c) Boundary condition and finite element mesh of soil box and furrow.

Figure 1 Cross-section, measured points, boundary condition and finite element mesh of the model

2.3 HYDRUS simulation

2.3.1 Modeling of nitrogen reactions

The HYDRUS-1D/2D can be used to simultaneously simulate reactions and transport of multiple solutes[21]. These solutes can be independent of each other or from the same first-order degradation reaction chain. Urea is initially hydrolyzed to form ammonium by urease in the soil, which is then nitrified by autotrophic bacteria to form nitrite and nitrate. This process can be described with the first-order decay chain as follows[7]:

$$(NH_2)_2CO \rightarrow NH_4^+ \rightarrow NO_2^- \rightarrow NO_3^- \begin{matrix} \nearrow N_2 \\ \searrow N_2O \end{matrix} \quad (NH_4^+ \uparrow \text{gas}) \tag{1}$$

Due to the faster rate of nitrification from nitrite to nitrate compared with the nitrification of ammonium, both nitrification reactions are typically considered together, thereby neglecting the nitrite species. Volatilization of ammonium was also neglected[7,22]. The following N transformation processes were simulated using HYDRUS in this study: 1) hydrolysis of urea to NH_4^+-N, 2) adsorption of NH_4^+-N, 3) nitrification of NH_4^+-N to NO_3^--N, and 4) denitrification losses of NO_3^--N.

2.3.2 Soil water movement model

Assuming the soil is a homogeneous and isotropic rigid porous medium, the air resistance plays an insignificant role in the liquid flow process, and the effects of temperature and evaporation on infiltration are negligible. The 1D and 2D governing flow equation of variably saturated soil water movement under these conditions can be expressed as a modified form of the Richards' equation:[21]

$$\frac{\partial\theta}{\partial t} = \left\{\frac{\partial}{\partial z}\left[K(h)\frac{\partial h}{\partial z}\right] - \frac{\partial K(h)}{\partial z}\right\} + d\left\{\frac{\partial}{\partial x}\left[K(h)\frac{\partial h}{\partial x}\right]\right\} \tag{2}$$

where, θ is the soil water content, cm^3/cm^3; t is the time, min; h is the soil water pressure head, cm; z is a vertical coordinate that is positive in a downward direction; and x is a lateral coordinate. The value of coefficient d is 0 or 1 and represents the dimension of the Equation (2). If d is 0, it represents the 1D governing flow equation of variably saturated soil water movement; otherwise it represents the 2D governing flow equation of variably saturated soil water movement. $K(h)$ is the unsaturated hydraulic conductivity, cm/min, which can be described using the van Genuchten–Mualem (VG-M) model[23]:

$$K(h) = \begin{cases} K_s S_e^l\left[1-\left(1-S_e^{1/m}\right)^m\right]^2, & h<0 \\ K_s, & h\geq 0 \end{cases} \tag{3}$$

$$S_e = \begin{cases} \dfrac{\theta-\theta_r}{\theta_s-\theta_r} = \dfrac{1}{\left(1+|\alpha h|^n\right)^m}, & h<0 \\ 1, & h\geq 0 \end{cases} \tag{4}$$

where, θ_r is the residual soil water content, cm^3/cm^3; θ_s is the soil saturated water content, cm^3/cm^3; m, n, α, and l are empirical parameters of the soil water characteristic curve, m=1–(1/n). l is usually equal to 0.5; K_S is the saturated hydraulic conductivity, cm/min; and S_e is the relative hydraulic conductivity, cm/min.

2.3.3 Soil solute transport model

HYDRUS can be used to numerically solve the convection-diffusion equation using finite elements in space and finite differences in time, which predicts the fate of components in soil liquid, solid, and gaseous phases. The equations include provisions for kinetic attachment/detachment of solute to the solid phase, and they can be thus used to simulate adsorptive solute (NH_4^+)[7].

$$\frac{\partial\theta C_1}{\partial t} = \frac{\partial}{\partial x}\left(\theta D_{xx}^w\frac{\partial C_1}{\partial x}+\theta D_{xz}^w\frac{\partial C_1}{\partial z}\right)+\frac{\partial}{\partial z}\left(\theta D_{zz}^w\frac{\partial C_1}{\partial z}+\theta D_{zx}^w\frac{\partial C_1}{\partial x}\right)-\left(\frac{\partial q_x C_1}{\partial x}+\frac{\partial q_z C_1}{\partial z}\right)-\mu_{w,1}\theta C_1 \tag{5}$$

$$\frac{\partial\theta C_2}{\partial t}+\frac{\partial\rho S_2}{\partial t} = \frac{\partial}{\partial x}\left(\theta D_{xx}^w\frac{\partial C_2}{\partial x}+\theta D_{xz}^w\frac{\partial C_2}{\partial z}\right)+\frac{\partial}{\partial z}\left(\theta D_{zz}^w\frac{\partial C_2}{\partial z}+\theta D_{zx}^w\frac{\partial C_2}{\partial x}\right)-\left(\frac{\partial q_x C_2}{\partial x}+\frac{\partial q_z C_2}{\partial z}\right)-\mu_{w,2}\theta C_2-\mu_{s,2}\rho S_2+\mu_{w,1}\theta C_1 \tag{6}$$

$$\frac{\partial\theta C_3}{\partial t} = \frac{\partial}{\partial x}\left(\theta D_{xx}^w\frac{\partial C_3}{\partial x}+\theta D_{xz}^w\frac{\partial C_3}{\partial z}\right)+\frac{\partial}{\partial z}\left(\theta D_{zz}^w\frac{\partial C_3}{\partial z}+\theta D_{zx}^w\frac{\partial C_3}{\partial x}\right)-\left(\frac{\partial q_x C_3}{\partial x}+\frac{\partial q_z C_3}{\partial z}\right)+\mu_{w,2}\theta C_2+\mu_{s,2}\rho S_2-\mu_{w,3}\theta C_3 \tag{7}$$

where, C_1, C_2, and C_3 are the concentration of urea, NH_4^+-N, and NO_3^--N in the liquid phase, g/cm^3, respectively; $\mu_{w,1}$ is the first-order urea hydrolysis rate constant; and $\mu_{w,2}$ and $\mu_{s,2}$ are the first-order nitrification rate constant of NH_4^+-N in liquid and solid (due to adsorption) phase, min^{-1}, respectively. $\mu_{w,3}$ is the first-order NO_3^--N denitrification rate constant, min^{-1}. q_x and q_z are the volumetric flux density in the horizontal and vertical direction (cm/min), respectively. D_{xx}, D_{xz}, and D_{zz} are components of the effective dispersion coefficient tensor, cm^2/min. S_2 is the NH_4^+-N concentration in the solid phase due to adsorption, g/g, assuming that the NH_4^+-N is instantaneously (equilibrium) adsorbed on the solid phase[7]. In the case of 1D infiltration, note that the terms representing the x-direction and xz-direction are ignored. S_2 can be described by a linear equation:

$$S_2 = K_d C_2 \tag{8}$$

where, K_d is the distribution coefficient, cm^3/g.

2.3.4 Initial and boundary conditions

The initial solute conditions were defined using the measured concentration of urea, NO_3^--N, and NH_4^+-N (Table 1). The IWC was defined as θ_r. The boundary conditions of the 1D vertical and 2D urea solution infiltration experiments and simulation are shown in Figure 1 a and c[11,24]. Moreover, a non-uniform finite element mesh was generated by HYDRUS-2D for 2D infiltration, with its sizes gradually increasing with distance from the boundary that interfaced with the water (Figure 1c) to accurately model large spatial gradients in soil water pressure heads caused by infiltrating water[25].

2.3.5 Parameter inverse solution procedure and evaluation

The HYDRUS implements a Marquardt-Levenberg parameter inversion technique for inverse soil hydraulic parameters, solute reaction parameters from measured soil water content, and soil solute (urea, NH_4^+-N, and NO_3^--N) concentrate data[22]. The inverse method is based on the minimization of a suitable objective function, which expresses the discrepancy between the observed and predicted values. The objective function is defined as the sum of squared residuals (SSQ)[2]:

$$SSQ = \sum_{j=1}^{M} v_j \sum_{i=1}^{N} w_{ij}\left[q_j^*(x,z,t_i) - q_j^*(x,z,t_i,b)\right]^2 \tag{9}$$

where, N represents the number of measurements for the jth measurement set (e.g., soil water contents and soil solute concentrations); $q_j^*(x,z,t_i)$ represents the measurement at time t_i, location x, and depth z; $q_j^*(x,z,t_i,b)$ represents the corresponding model prediction value obtained with the vector of optimized parameters b (e.g., θ_r, θ_s, α, n, and K_s); and v_j and w_{ij} are the weights associated with a particular measurement set or point, respectively.

Weighting coefficients were assumed to be equal to 1 in all cases, representing that all data carried equal significance during the HYDRUS inversion process. The soil hydraulic parameters of the VG-M model were inversed by measured cumulative infiltration and soil water content at the end of the infiltration.

The HYDRUS-1D can estimate the hydrolysis rate constant for urea hydrolysis ($\mu_{w,1}$) by utilizing the measured urea content at various observation points of the 1D vertical urea solution infiltration experiment. Genetic algorithms (GA) have been widely used in modeling different water resources engineering parameter optimization problems[26]. In this study, the GA and the HYDRUS-1D were combined to determine the optimal value of the distribution coefficient (K_d), nitrification rate constant for ammonium nitrogen ($\mu_{w,2}$, $\mu_{s,2}$), and denitrification rate constant for nitrate ($\mu_{w,3}$). The main flowchart of parameter optimization is shown in Figure 2.

Quality in soil hydraulic and solute reaction parameters inversion and HYDRUS simulation was assessed using the root mean square error (RMSE), mean bias error (MBE), and coefficient of determination (R^2) between measured and estimated values[5].

2.4 Structural equation modeling

To understand the direct and indirect effects of the factors on the soil water and solute distribution characteristic of furrow irrigation, structural equation modeling (SEM) was used. The total effects of factors are the sum of direct and indirect path coefficients. The indirect effects were calculated by multiplying the path coefficients of factors in SEM[27]. The analyses and SEM were performed using the lavaan package in *R*[28]. The reliability of the SEM was evaluated with the following indicators: Chi-square, standardized root mean square residual (SRMR), comparative fit index (CFI), *p*-value of the model, the degrees of freedom (*Df*), and root mean square error of approximation (RMSEA). The *p*-value of the models>0.05, CFI>0.95, RMSEA<0.06, SRMR<0.09, and Chi-square/*Df*<3, indicating the model fit well and is reliable for the data[27,29].

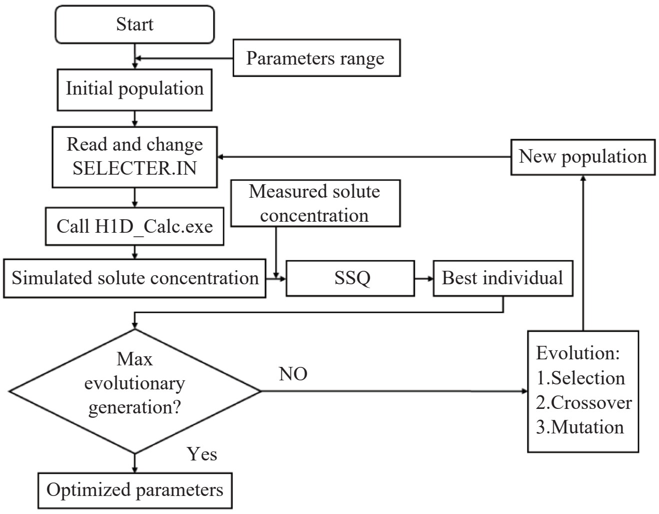

Figure 2 Flowchart of parameter optimization

3 Results and analysis

3.1 Parameter inversion and verification

3.1.1 Soil hydraulic parameters

Through the HYDRUS-1D, the soil hydraulic parameters were inversed based on the cumulative infiltration and the soil water content at the measured points obtained from a 1D vertical urea solution infiltration experiment conducted on clay loam and sandy loam (Figure 1a). The parameter θ_r in Equation (4) is often considered an empirical fitting parameter that is not sensitive to changes in the shape of the soil water characteristic curve (SWCC)[11,30]. Thus, the θ_r was approximated for air-dried soil water content (0.035 and 0.023 cm³/cm³ for clay and sandy loam soils, respectively) during the inverse solution. The inversion results of other soil hydraulic parameters (i.e., θ_s, α, n, and K_s) and the errors (SSQ and R^2) of clay and sandy loam soils under various urea solution concentration treatments are listed in Table 2.

Table 2 Inversed soil hydraulic parameters and errors for clay loam and sandy loam during the inverse process

Treatment	Clay loam						Sandy loam					
	Soil hydraulic parameters				Errors		Soil hydraulic parameters				Errors	
	θ_s/cm³·cm⁻³	α	n	K_s/cm·min⁻¹	*SSQ*	R^2	θ_s/cm³·cm⁻³	α	n	K_s/cm·min⁻¹	*SSQ*	R^2
CK	0.4330	0.0003	1.1912	0.0009	0.7980	0.9996	0.3170	0.0154	1.2010	0.0220	0.1770	0.9971
T1	0.4390	0.0004	1.2240	0.0010	0.1878	0.9991	0.3360	0.0224	1.2960	0.0246	0.1980	0.9981
T2	0.4450	0.0006	1.2250	0.0016	0.5220	0.9996	0.3400	0.0255	1.3000	0.0257	0.1200	0.9988
T3	0.4510	0.0009	1.2390	0.0023	0.4890	0.9995	0.3500	0.0268	1.4000	0.0281	0.3150	0.9989
T4	0.4560	0.0011	1.2760	0.0023	0.4120	0.9993	0.3540	0.0320	1.4500	0.0283	0.1120	0.9991
T5	0.4640	0.0014	1.2850	0.0026	0.6770	0.9991	0.3600	0.0331	1.5540	0.029	0.2430	0.9991
T6	0.4730	0.0019	1.3090	0.0033	0.1080	0.9985	0.3600	0.0354	1.5970	0.0307	0.4960	0.9988
T7	0.4800	0.0025	1.3800	0.0043	0.6340	0.9972	0.3650	0.0382	1.6500	0.0342	0.2050	0.9966

Note: θ_s, α, n, and K_S are the parameters of the van Genuchten–Mualem model, respectively; *SSQ* is the sum of squared residuals; R^2 is the coefficient of determination.

The inversed parameters were input into HYDRUS-2D to simulate the clay loam and sandy loam (IWC=θ_r) of furrow urea solution infiltration process and the soil water content at the end of the infiltration experiment under urea solution concentrations of 0, 0.4, 0.8, 1, 3, and 5 g/L (CK, T2, T4, T5, T6, and T7). The mean values of the RMSE, MBE, and R^2 between the measured and simulated cumulative infiltration and soil water content of clay loam soil (sandy loam soil) at different urea concentrations were 0.3176 (0.2700) cm, –0.0584 (0.0168) cm, 0.9950 (0.9967) and 0.0449 (0.0309) cm³/cm³, –0.0027 (–0.0038) cm³/cm³, 0.8729 (0.8604), respectively. These errors were similar to the reported studies[11,31], indicating that the soil hydraulic parameters were reliable in furrow irrigation process simulation.

3.1.2 Solute reaction parameters

The first-order urea hydrolysis rate constants ($\mu_{w,1}$), first-order nitrification rate constant ($\mu_{w,2}$, $\mu_{s,2}$) of NH_4^+-N, denitrification rate constant ($\mu_{w,3}$) of NO_3^--N, and distribution coefficient (K_d) were determined using HYDRUS-1D and GA. This determination was based on the inversed soil hydraulic parameters (Table 2) and measured solute concentration at days 0, 1, 3, 5, and 10 following the conclusion of 1D vertical urea solution infiltration experiments. The results and errors are listed in Table 3.

Table 3 Inversed solute reaction parameters and errors during the inverse process

Solute reaction parameters	Clay loam			Sandy loam		
	Values	SSQ/g·cm^{-3}	R^2	Values	SSQ/g·cm^{-3}	R^2
$\mu_{w,1}$/min^{-1}	5.420×10^{-4}	3.491×10^{-10}	0.9969	4.640×10^{-4}	3.482×10^{-10}	0.9967
K_d/cm^3·g^{-1}	2.969			1.890		
$\mu_{w,2}$/min^{-1}	7.776×10^{-5}	4.319×10^{-11}	0.9971	1.524×10^{-4}	2.834×10^{-12}	0.9950
$\mu_{s,2}$/min^{-1}	7.776×10^{-5}			1.524×10^{-4}		
$\mu_{w,3}$/min^{-1}	3.865×10^{-6}	1.633×10^{-11}	0.9945	1.536×10^{-6}	1.089×10^{-11}	0.9893

Note: $\mu_{w,1}$ is the first-order rate constant of urea hydrolysis; $\mu_{w,2}$, and $\mu_{s,2}$ are the first-order nitrification rate constants of NH_4^+-N in water and solid phase, respectively; $\mu_{w,3}$ is the first-order denitrification rate constant; and K_d is the distribution coefficient.

The solute reaction parameters inversed through 1D vertical urea solution infiltration experiments were also used to simulate the 2D furrow solute transport process to evaluate the reliability of the parameters. The mean values of the RMSE, MBE, and R^2 between the measured and simulated solute concentrations (CK, T2, T4, T5, T6, and T7) of urea, NH_4^+-N, and NO_3^--N in clay loam soil (sandy loam soil) were 0.1188 mg/cm^3, –0.0239 mg/cm^3, and 0.9544 (0.1216 mg/cm^3, –0.0128 mg/cm^3, and 0.9564), 0.0052 mg/cm^3, 0 mg/cm^3, and 0.9356 (0.0061 mg/cm^3, 0.0001 mg/cm^3, and 0.9164), 0.0966 mg/cm^3, 0.0198 mg/cm^3, and 0.9381 (0.0819 mg/cm^3, 0.0252 mg/cm^3, and 0.9379), respectively. Meanwhile, the RMSE, MBE, and R^2 of the measured and simulated concentration of urea, NH_4^+-N, and NO_3^--N at different treatments were acceptable and varied within ranges similar to those reported in previous studies[2,11,31], indicating that the solute reaction parameters were reliable in furrow irrigation process simulation.

3.2 Analysis of soil water and solute transport characteristics under different furrow irrigation conditions

3.2.1 Urea solution concentration

Due to the similarity in the simulation results of soil water and nitrogen transport between clay loam and sandy loam under different conditions, clay loam was used as an example for explanation. The distributions of the soil water, urea, NH_4^+-N, and NO_3^--N in clay loam soil at different urea concentrations (C=0.4, 1, and 5 g/L) was simulated based on the following conditions: soil initial water content (IWC) of 0.128 cm^3/cm^3 (40% of FC), water depth (WD) of 10 cm, soil bulk density of 1.35 g/cm^3, and furrow bottom width (FW) of 20 cm (Figure 3).

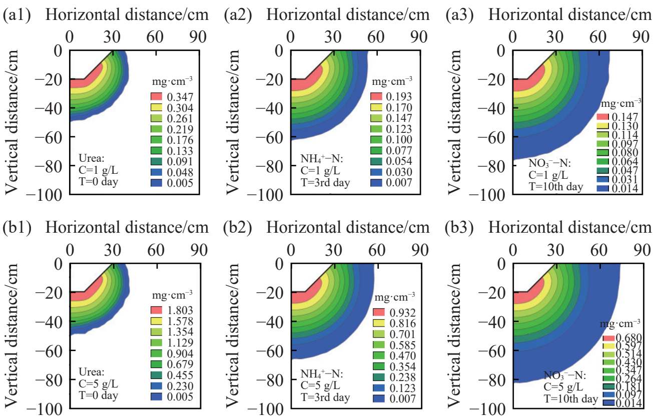

Note: (a1-a3) 1g/L, (b1-b3) 5g/L

Figure 3 Distribution characteristics of urea, NH_4^+-N, and NO_3^--N under different urea concentrations

When the cumulative infiltration reached 80 mm in clay loam, the infiltration time for simulation at C=0.4 g/L was 248.8 min, significantly longer than those at C=1 g/L and C=5 g/L, by 6.10% and 25.78%, respectively. The infiltration rate increased with urea concentration C, attributed to urea hydrolysis producing NH_4^+ with strong adsorption and soil structure-altering ability, enhancing soil infiltration capacity[5]. The urea concentration slightly influenced the wetting pattern at the end of the infiltration, but the distribution range of the wetting pattern increased with increasing urea concentration in the redistribution process (Figure 3). The results showed that the vertical and horizontal distribution distances of the NH_4^+-N in clay soil on the 3rd day in the redistribution process at urea concentration of 5g/L were longer than those of the simulations at C=0.4 g/L and C=1 g/L by 10.14%, 8.59% and 10.45%, 7.72%, respectively. However, the distribution range of the NH_4^+-N was less than that of the soil water and NO_3^--N. This result can be attributed to the adsorption of NH_4^+.

Figure 4 shows the vertical distributions of urea, NH_4^+-N, and NO_3^--N contents at the end of infiltration and during the redistribution process (0-10 d) at C=1 g/L. Urea content decreased with soil depth and distribution time (Figure 4a) due to continuous hydrolysis into NH_4^+-N by urease, and was almost completed on the 5th day. During redistribution, NH_4^+-N content increased to a maximum on the 3rd day and then decreased, as hydrolysis dominated initially but nitrification surpassed hydrolysis after the 3rd day (Figure 4b). NO_3^--N content was initially lower than the initial value and then increased above it, reaching a maximum at the wetting front at the end of infiltration (Figure 4c). This was because nitrification of NH_4^+-N was low during infiltration, replenishing a small amount of NO_3^--N. As NO_3^- cannot be adsorbed, urea solution leached NO_3^--N, resulting in concentrated distribution at the wetting front. NO_3^--N content increased with distribution time due to continuous nitrification from NH_4^+-N (Figure 4c), with a higher nitrification rate constant than denitrification rate constant of NO_3^--N.

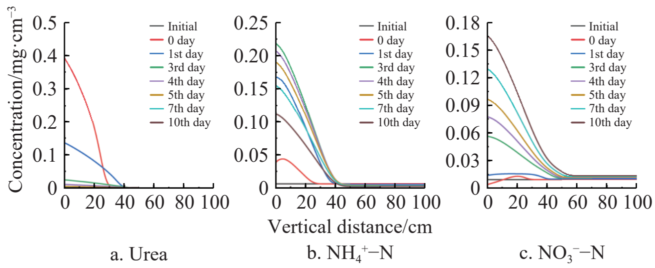

Figure 4 Redistribution of solutes under urea concentration of 1 g/L

3.2.2 Water depth

The distributions of the soil water, urea, NH_4^+-N, and NO_3^--N in clay loam at C=1 g/L were simulated under the following conditions: IWC=0.128 cm^3/cm^3 (40% of FC), soil bulk density of 1.35 g/cm^3, FW=20 cm, and WD of 5, 10, and 15 cm (Figure 5).

The results showed that the infiltration rate increased with increasing WD, and the infiltration times for simulation with WD=5 cm were 300 min, which was considerably longer than those of simulation with WD=10 cm and WD=15 cm, by 52.14% and 115.05%, respectively. The main reason was that the increase in WD increased the infiltration perimeter and infiltration area of the furrow. At the end of infiltration, the wetting patterns under different WDs (5, 10, and 15 cm) revealed that the vertical distribution range of soil water, urea, NH_4^+-N, and NO_3^--N decreased with increasing WD, while the horizontal distribution range increased (Figure 5). Specifically, the vertical distribution distance of soil water under WD=5 cm was greater than that under WD=10 cm and WD=15 cm by 7.42% and 16.7%, respectively.

Conversely, the horizontal distribution distance under WD=15 cm was greater than that under WD=10 cm and WD=5 cm by 20.14% and 51.33%, respectively. On the 3rd day, the vertical distance of NH_4^+-N under WD=5 cm was greater than that under WD=10 cm and WD=15 cm by 4.72% and 8.19%, respectively. Similarly, on the 10th day, the horizontal distribution distance of NO_3^--N under WD=15 cm was greater than that under WD=10 cm and WD=5 cm by 6.49% and 15.65%, respectively.

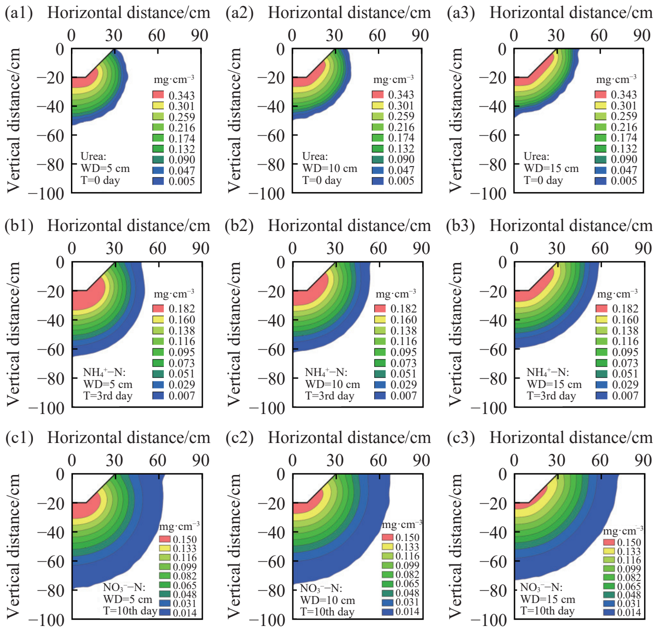

Note: (a1-a3) urea, (b1-b3) NH_4^+-N, (c1-c3) NO_3^--N.

Figure 5 Distribution of urea, NH_4^+-N, and NO_3^--N under urea concentration of 1 g/L at WD of 5, 10, and 15 cm, respectively

3.2.3 Furrow bottom width

The distributions of the soil water, urea, NH_4^+-N, and NO_3^--N of clay loam were simulated under the following conditions: soil IWC of 0.128 cm³/cm³ (40% of FC), WD=10 cm, C=1g/L, soil bulk density of 1.35 g/cm³, and FW of 10, 20, and 30 cm (Figure 6).

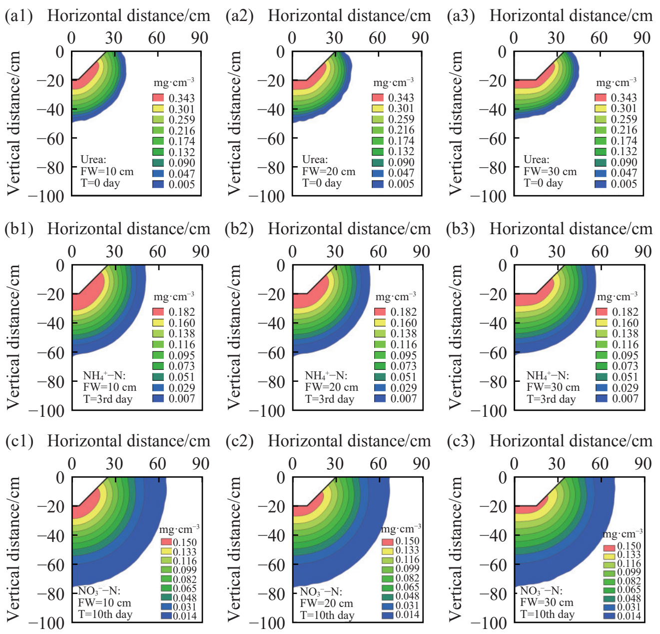

Note: (a1-a3) urea, (b1-b3) NH_4^+-N, (c1-c3) NO_3^--N.

Figure 6 Distribution of urea, NH_4^+-N, and NO_3^--N under urea concentration of 1 g/L for FW of 10, 20, and 30 cm, respectively

Similar to the influence of WD on the infiltration time, the increase in FW increased the infiltration perimeter and infiltration area of the furrow, thus decreasing infiltration time when the cumulative infiltration was 80 mm in the clay loam. The infiltration time for the simulation with FW=10 cm was 379.5 min, which is considerably longer than those of the simulation with FW=20 cm and FW=30 cm, by 65.72% and 107.72%, respectively. The results show that increasing the FW enhances the horizontal distribution range of the soil water, urea, NH_4^+-N, and NO_3^--N while reducing their vertical distribution range (Figure 6). For instance, the horizontal distance distributions of the soil water content of clay soil at the end of infiltration under FW=30 cm were larger than those under WD=20 cm and WD=10 cm by 8.01% and 18.66%, respectively. The horizontal distance distributions of the NH_4^+-N of clay soil on the 3rd day during the redistribution process under FW=30 cm were larger than those under FW=20 cm and FW=10 cm by 6.54% and 11.08%, respectively. For the distribution of NO_3^--N, the horizontal distance distributions of clay soil on the 10th day under FW=30 cm were larger than those under FW=20 cm and FW=10 cm by 7.72% and 4.99%, respectively. This phenomenon is because the increase in FW mainly increased the distance between the wetting front in the horizontal direction and the center of the furrow and increased the infiltration area along the furrow bottom.

3.2.4 Soil initial water content

The distributions of the soil water, urea, NH_4^+-N, and NO_3^--N of clay loam were simulated under the following conditions: WD=10 cm, soil bulk density of 1.35 g/cm³, FW=20 cm, C=1g/L, and IWC of 0.128, 0.176, and 0.208 cm³/cm³ (i.e., 40%, 55%, and 65% of FC). Increasing IWC prolongs the time to reach a cumulative infiltration of 80 mm, unlike the enhancing effects of C, WD, and FW. For simulations with IWC=0.208 cm³/cm³, the infiltration times (281 min) were 8.91% and 22.71% longer than those with IWC=0.176 and 0.128 cm³/cm³, respectively. The results show that the distribution range of soil water, urea, NH_4^+-N, and NO_3^--N increased with the increase of IWC, and IWC had a more pronounced effect during redistribution (Figure 7). For instance, the vertical distance distributions of soil water at the end of infiltration under IWC=0.208 cm³/cm³ were 4.98% and 9.83%, larger than those under IWC=0.176 cm³/cm³ and 0.128 cm³/cm³, respectively. On the 3rd day of redistribution, these increases were 45.43% and 60.6%, respectively. In the horizontal direction, the relative increases were 18.31% and 38.73%. This phenomenon is because as the IWC of soil becomes relatively high, the soil rapidly becomes saturated, thus accelerating the wetting front movement[11]. Additionally, the distribution ranges of urea, NH_4^+-N, and NO_3^--N in clay loam soil increased with IWC during infiltration and redistribution (Figure 7).

Increasing IWC prolongs the time to reach a cumulative infiltration of 80 mm, unlike the enhancing effects of C, WD, and FW. For simulations with IWC=0.208 cm³/cm³, the infiltration time (281 min) was 8.91% and 22.71% longer than those with IWC=0.176 and 0.128 cm³/cm³, respectively. The results show that the distribution range of soil water, urea, NH_4^+-N, and NO_3^--N increased with the increase of IWC, and IWC had a more pronounced effect during redistribution (Figure 7). For instance, the vertical distance distributions of soil water at the end of infiltration under IWC=0.208 cm³/cm³ were 4.98% and 9.83%, larger than those under IWC=0.176 cm³/cm³ and 0.128 cm³/cm³, respectively. On the 3rd day of redistribution, these increases were 45.43% and 60.6%, respectively. In the horizontal direction, the relative increases were 18.31% and 38.73%. This phenomenon is because as the IWC of soil becomes relatively high, the soil rapidly becomes saturated, thus accelerating the wetting front movement[11]. Additionally, the distribution ranges of urea, NH_4^+-N, and NO_3^--N in clay loam soil increased with IWC during infiltration and redistribution (Figure 7).

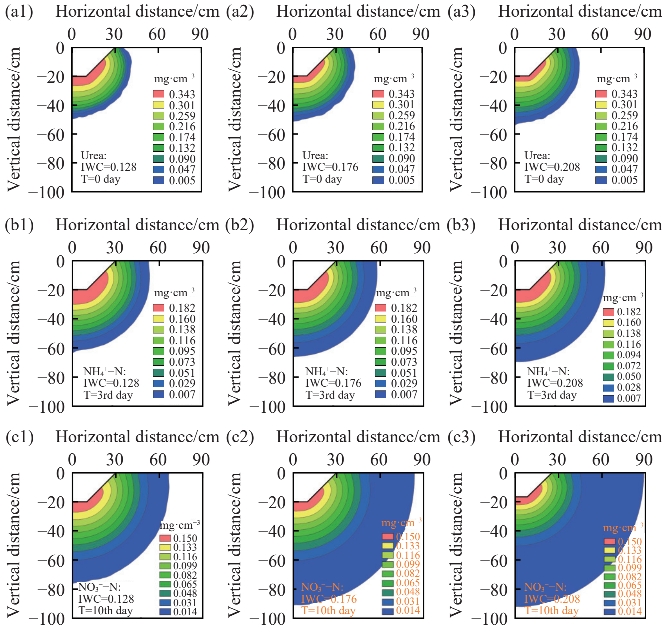

Note: (a1-a3) urea, (b1-b3) NH_4^+-N, (c1-c3) NO_3^--N.

Figure 7 Distribution of urea, NH_4^+-N, and NO_3^--N under urea concentration of 1 g/L for soil IWC of 0.128, 0.176, and 0.208 cm³/cm³, respectively

With the increase in IWC, the soil water content in the soil wetting pattern also increased, and the influence of IWC on soil water content was more significant in the redistribution process. For example, the mean value of soil water content under IWC=0.208 cm³/cm³ was 0.396 cm³/cm³, which was larger than that of simulation under IWC=0.176 cm³/cm³ and IWC=0.128 cm³/cm³ by 0.3% and 3.9% at the end of infiltration, respectively. However, compared with the increase in soil water content with IWC, the solute (urea, NH_4^+-N, and NO_3^--N) content in the soil wetting pattern decreased with the increase in IWC. For instance, compared with the simulation of IWC=0.176 cm³/cm³ and IWC=0.208 cm³/cm³, the relative increases in the mean value of urea content of simulation under IWC=0.128 cm³/cm³ were 11.57% and 22.61% at the end of infiltration. This increment is attributed to the same cumulative infiltration, and the mass of solute that enters the soil at the end of infiltration is the same at different IWC values. However, the increase in IWC expands the distribution range of the solute, thereby reducing the concentration of solute in the wetting pattern under higher soil initial water content conditions.

3.3 SEM between soil water, solute transportation, and different influential factors

To quantitatively analyze the effect of the factors (C, WD, FW, and IWC) on the soil water and solute transport characteristics under furrow irrigation, the wetting pattern was divided into horizontal (H) and vertical (V) parts. The vertical (V) part is the wetting pattern under the furrow bottom (i.e., under the DE boundary in Figure 1b), and the rest is the horizontal (H) part. To reduce the risk of water-deep drainage and NO_3^--N leaching, the wetting pattern should have a larger ratio of horizontal and vertical transporting distance of the wetting front (X(H/V)). Hence, the C, WD, FW, and IWC were considered as exogenous variables. In addition, the total content of soil water (Water (H)), the total content of soil NO_3^--N (NO_3^--N(H)) in the horizontal (H) part, the horizontal transporting distance of the wetting front (X(H)), the X(H/V), and infiltration time (T) were considered as endogenous variables to quantitatively analyze the effects of factors on the distribution of soil water and solute using SEM. The IWC was set as 40%, 46%, 52%, 58%, and 65% of FCs[32,33]; the WD in furrow were set as 5, 7.5, 10, 12.5, and 15 cm[1,34]. The FW values were changed to 10, 15, 20, 25, and 30 cm[1,35] to simulate the soil water and solute transport of furrow irrigation at concentrations of 0.4, 0.8, 1, 3, and 5 g/L. The SEM was finally established based on simulated data on the 5th day (as a representative), because urea is not directly absorbable as a nutrient by plants, and was basically hydrolyzed into NH_4^+-N by urease (Figure 4). The SEM is shown in Figure 8.

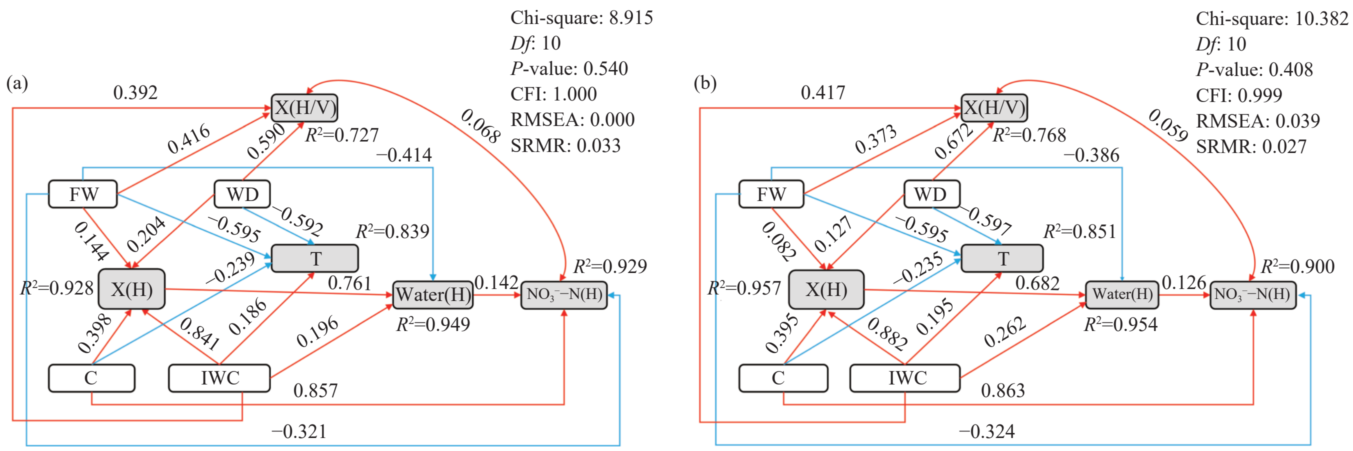

Note: Df is the degrees of freedom, CFI is a comparative fit index, RMSEA is the root mean square error of approximation, and SRMR is the standardized root mean square residual. X(H) is the horizontal transporting distance of the wetting front, and X(H/V) is the ratio of the horizontal and vertical transporting distance of the wetting front.

Figure 8 SEM representing connections between various factors and distribution characteristics of soil water and solute for (a) clay loam and (b) sandy loam

The SEM revealed that the WD, FW, and C had direct and negative effects on the infiltration time, and the IWC positively and directly influenced the infiltration time. The WD, FW, and IWC directly affected the X(H/V). Among the factors, the WD had the largest effect on X(H/V), with coefficients of 0.590 and 0.672 for clay loam and sandy loam, respectively. This phenomenon is because the WD, FW, and IWC positively affect the X(H) (Figure 8). Although the IWC had the largest effect on X(H), the WD had the largest effect on X(H/V). This phenomenon may be because the increase in WD increases X(H) and decreases the vertical transporting distance of the wetting front (X(V)) (Figure 5). Moreover, the increasing IWC increases both X(H) and X(V) according to the results in the above sections.

The interactions among the X(H), Water(H), and NO_3^--N(H) were also analyzed using SEM. The X(H) directly and positively affected the Water(H) (Figure 8), and the Water(H) directly and positively affected the NO_3^--N (H). The X(H) indirectly affected the NO_3^--N (H) through the Water(H), with path coefficients of 0.108 and 0.086 for clay loam and sandy loam, respectively. Additionally, IWC and FW directly affected Water(H) among the four factors (*C*, WD, FW, and IWC), but the *C* and WD had no direct effect on Water(H) (Figure 8). Furthermore, the results indicated that the FW directly and negatively affected the NO_3^--N(H) among the four factors (*C*, WD, FW, and IWC), with path coefficients of –0.321 and –0.324 for clay loam and sandy loam, respectively; and the *C* directly and positively affected the NO_3^--N(H), with path coefficients of 0.857 and 0.863 for clay loam and sandy loam, respectively. The IWC, *C*, WD, and FW also indirectly influenced the NO_3^--N(H) through the X(H) and Water(H) (Figure 8), with path coefficients of 0.091, 0.043, 0.022, and 0.015 for clay loam and 0.106, 0.034, 0.011, and 0.007 for sandy loam, respectively. The total effect of the IWC on the NO_3^--N(H) was 0.900 and 0.897 for clay loam and sandy loam, respectively. The total effect of the FW on the NO_3^--N(H) was –0.306 and –0.317 for clay loam and sandy loam, respectively. This result confirms that the increases in the IWC, WD, and *C* increase the NO_3^-s-N(H). Conversely, higher FW leads to a decrease in NO_3^--N(H).

4 Discussion

4.1 Determination of soil hydraulic and solute reaction parameters

Accurately determining soil hydraulic parameters (e.g., θ_r, θ_s, α, n, and K_s) and solute reaction parameters using appropriate methods is the basis for effectively simulating water and nutrient transport in soil. This study determined soil hydraulic parameters under various urea solutions using 1D vertical infiltration experiment data by HYDRUS. The verified results showed the mean value of the RMSE, MBE, and R^2 between the measured and simulated cumulative infiltration and soil water content of clay loam soil and sandy loam soil were similar to the reported studies[2,11,31]. This indicated that the soil hydraulic parameters were reliable in furrow irrigation process simulation. The HYDRUS cannot simultaneously inverse the reaction parameters for the three solutes (urea, NH_4^+-N, and NO_3^--N) of the urea first-order decay chain, especially in variably saturated flow[13]. Ranjbar et al.[17] simulated the nitrogen uptake and distribution of furrow irrigation during the maize growth period using HYDRUS-2D. The nitrification rate constant of urea and ammonium nitrogen ($\mu_{w,1}$, $\mu_{w,2}$, $\mu_{s,2}$) was determined using the trial and error method. However, this method is time-consuming and labor-intensive. In this study, the first-order urea hydrolysis rate constants ($\mu_{w,1}$) were inversed using HYDRUS first. Then, the first-order nitrification rate constant ($\mu_{w,2}$, $\mu_{s,2}$) of NH_4^+-N, denitrification rate constant ($\mu_{w,3}$) of NO_3^--N, and distribution coefficient (K_d) were determined by combining GA and HYDRUS-1D based on the inversed soil hydraulic parameters and the measured solute concentration during the distribution process. The verification results show that the mean values of the RMSE, MBE, and R^2 between the measured and simulated solute concentrations (CK, T2, T4, T5, T6, and T7) of urea, NH_4^+-N, and NO_3^--N in soil and sandy loam soil were acceptable and varied within ranges similar to those reported in previous studies[2,11,31]. These results indicate that the solute reaction parameters were reliable in furrow irrigation process simulation, and the combination of GA and HYDRUS is an effective strategy to determine the solute reaction parameters in the decay chain.

4.2 Modeling furrow irrigation using the parameters determined through the one-dimensional vertical infiltration experiment

The 2D problem is more complicated than the 1D problem in terms of accuracy, cost, and time issues[2]. Moreover, conducting 2D experiments is challenging and requires more work intensity compared with 1D experiments. Several studies have attempted to simplify a 2D problem into a 1D problem. Tafteh and Sepaskhah[14] used HYDRUS-1D to simulate water and nitrate leaching at different nitrogen fertilization rates (as urea) under furrow irrigation. They confirmed that HYDRUS-1D was able to simulate deep percolation of soil water and NO_3^--N leaching with outstanding accuracy. The soil water and solute transport in deeper soil profiles might be dominated by gravitational flow, which may be described using HYDRUS-1D[14]. However, the transfer of soil water and solute in furrow irrigation is 2D, which may not be simplified into a 1D problem under many complex situations. In this study, the soil hydraulic parameters and solute reaction parameters determined based on vertical urea solution infiltration experiments were used in HYDRUS-2D to simulate the urea solution infiltration and decay process of furrow irrigation, and the errors between the measured and simulated values of soil water and solute were acceptable. This may be because when the soil is a homogeneous and isotropic rigid porous medium, and the water above it is essentially still during the infiltration, the soil hydraulic parameters and solute reaction parameters are independent of the spatial dimensions of soil samples. These parameters are mainly correlated to soil texture, bulk density, and soil structure. The results confirmed that the required parameters for HYDRUS-2D were determined based on HYDRUS-1D. Describing 2D problems using HYDRUS-2D is an efficient and feasible strategy, which can ensure a balance between cost and reliability in simplifying a 2D problem into a 1D problem.

4.3 Soil water and solute transport characteristics under different furrow irrigation conditions

The results showed that the urea solution concentration (*C*) had obvious influence on the soil water and solute distribution range in the redistribution process. Meanwhile, the inversed parameter values of α and n in the VG-M model increased with the *C* for both clay loam and sandy loam (Table 2). This phenomenon may be because the NH_4^+ hydrolyzed from the urea increases the volume of macro pores[4,5], thus decreasing the water retention capacity and increasing the water infiltration capacity of the soil. Finally, the distribution range of water, urea, NH_4^+-N, and NO_3^--N simultaneously increased with the urea concentration.

The SEM revealed that WD and FW significantly and positively influenced the X(H/V). The IWC also positively affected the X(H) and X(H/V), because it made the soil saturated faster, and this feature increased the wetting front movement distance, thus increasing X(H) and X(H/V)[11]. However, the positive influence of IWC in soil water and the solute distribution range were observed in both vertical and horizontal directions. An increase in the IWC can also increase the risk of the deep drainage of water and NO_3^--N leaching. Therefore, fertigation should be conducted when the IWC is low, even if the IWC positively affects the X(H), X(H/V), water(H), and NO_3^--N(H). The *C* had a direct effect on NO_3^--N(H) but no effects on the X(H/V), which may be because *C* influenced soil water and the solute distribution range in both vertical and horizontal directions. Moreover, increase in *C* can also increase the volume of soil macro pores, as well as the risk of the deep drainage of water and NO_3^--N leaching. Therefore, suitable urea solution concentration and fertigation strategies should be taken in furrow irrigation. For instance, the strategy of first applying water for approximately half of the total irrigation time and then applying fertilizer solution for approximately half of the total irrigation time may reduce the risk of the deep drainage of water and NO_3^--N leaching[36–38]. According to the results of this study, it is suggested that WD and FW should be appropriately increased during furrow irrigation to increase the horizontal distribution of NO_3^--N. To reduce the risk of deep leaching of NO_3^--N, farmers should avoid fertigation when the soil water content is high in the range of suitable water contents for crop growth.

5 Conclusions

In this study, the column infiltration experiment and 2D furrow infiltration experiment were conducted using clay loam and sandy loam soils under multiple urea solution concentrations. Soil hydraulic and solute reaction parameters were inversed through the column infiltration experiment to explore the soil water and solute transport characteristics under different furrow irrigation conditions. The following conclusions were drawn from the study:

1) The soil hydraulic parameters and solute reaction parameters inversed by HYDRUS-1D and GA through 1D urea solution infiltration experiments were reliable in simulating the soil water movement and urea hydrolysis process of furrow irrigation during infiltration and distribution after infiltration. Moreover, the solute reaction parameters in the decay chain were effectively determined using a combined strategy of GA and HYDRUS.

2) The urea in the soil profile was completely hydrolyzed on the 5th day of the redistribution process. The NO_3^--N content in the soil profile increased with the distribution time, and the NH_4^+-N content initially increased to the maximum value on the 3rd day of the redistribution process and then decreased. The distribution of urea and NO_3^--N nitrogen had a similar trend with soil water, and the distribution range of the NH_4^+-N was less than that of the soil water. The nitrogen (urea, NH_4^+-N, and NO_3^--N) content in soil decreased with both vertical and horizontal distance.

3) The infiltration rate of furrow irrigation increased with *C*, WD, and FW but decreased with IWC. The distribution range of soil water and nitrogen increased with *C* and IWC, and an increase in WD and FW mainly increased the horizontal distribution range of the soil water and nitrogen. The SEM revealed that the IWC, FW, and WD had positive effects on the X(H/V), among which WD had the maximal effect, with coefficients of 0.590 and 0.672 for clay loam and sandy loam, respectively. The WD and FW should be appropriately increased during furrow irrigation. Additionally, to reduce the risk of deep leaching of NO_3^--N, fertigation should be avoided when the soil water content is high in the range of suitable water contents for crop growth.

Acknowledgements

This research was supported by the National Natural Science Foundation of China (Grant No. 52279043), the Key Research and Development Program of Shaanxi (Grant No. 2024NC-YBXM-243), and the Science and Technology Program of Xi'an (Grant No. 24NYGG0097).

[References]

[1] Nie W B, Feng Z J, Li Y B, Zhang F, Ma X Y. Determining a reasonable distance of collecting irrigation data for real-time management of furrow irrigation. Irrigation and Drainage, 2022; 71(5): 1208–1224.

[2] Ebrahimian H, Liaghat A, Parsinejad M, Abbasi F, Navabian M. Comparison of one- and two-dimensional models to simulate alternate and conventional furrow fertigation. Journal of Irrigation and Drainage Engineering, 2012; 138(10): 929–938.

[3] Karandish F, Šimůnek J. Two-dimensional modeling of nitrogen and water dynamics for various n-managed water-saving irrigation strategies using hydrus. Agricultural Water Management, 2017; 193: 174–190.

[4] Yu Z H, Li H, Liu X M, Xu C Y, Xiong H L. Influence of soil electric field on water movement in soil. Soil and Tillage Research, 2016; 155: 263–270.

[5] Feng Z J, Nie W B, Ma Y P, Li Y, Ma X Y, Zhu H Y. Effects of urea solution concentration on soil hydraulic properties and water infiltration capacity. Science of The Total Environment, 2023; 898: 165471.

[6] Tuo Y F, Shen F Y, Yang C P, Zhang L, Wang F, Wang Q, et al. Effect of urea fertilizer concentration on water and nitrogen transport and transformation in soil in a film - hole multi - line interference infiltration system*. Irrigation and Drainage, 2021; 70(4): 634–643.

[7] Hanson B R, Šimůnek J, Hopmans J W. Evaluation of urea–ammonium–nitrate fertigation with drip irrigation using numerical modeling. Agricultural Water Management, 2006; 86(1): 102–113.

[8] Abbasi F, Adamsen F J, Hunsaker D J, Feyen J, Shouse P, van Genuchten M Th. Effects of flow depth on water flow and solute transport in furrow irrigation: field data analysis. Journal of Irrigation and Drainage Engineering, 2003; 129(4): 237–246.

[9] Ebrahimian H, Liaghat A, Parsinejad M, Playán E, Abbasi F, Navabian M. Simulation of 1D surface and 2D subsurface water flow and nitrate transport in alternate and conventional furrow fertigation. Irrigation Science, 2013; 31(3): 301–316.

[10] Šimůnek J, Bristow K L, Helalia S A, Siyal A A. The effect of different fertigation strategies and furrow surface treatments on plant water and nitrogen use. Irrigation Science, 2016; 34(1): 53–69.

[11] Nie W B, Nie K K, Li Y B, Ma X Y. HYDRUS-2D simulations of nitrate nitrogen and potassium transport characteristics under fertilizer solution infiltration of furrow irrigation. Water Supply, 2020; 21(6): 2665–2680.

[12] Singh B, Singh B, Singh Y. Urease activity and kinetics of urea hydrolysis in some soils from semiarid regions of northwestern india. Arid Soil Research and Rehabilitation, 1992; 6(1): 21–32.

[13] Simunek J Jirka, van Genuchten M Th, Šejna M. HYDRUS: model use, calibration, and validation. Transactions of the ASAE. American Society of Agricultural Engineers, 2012; 55: 1261–1274.

[14] Tafteh A, Sepaskhah A R. Application of hydrus-1D model for simulating water and nitrate leaching from continuous and alternate furrow irrigated rapeseed and maize fields. Agricultural Water Management, 2012; 113: 19–29.

[15] Rodríguez S B, Alonso-Gaite A, Álvarez-Benedí J. Characterization of nitrogen transformations, sorption and volatilization processes in urea fertilized soils. Vadose Zone Journal, 2005; 4(2): 329–336.

[16] Mo X Y, Peng H, Xin J, Wang S. Analysis of urea nitrogen leaching under high-intensity rainfall using hydrus-1D. Journal of Environmental Management, 2022; 312: 114900.

[17] Ranjbar A, Rahimikhoob A, Ebrahimian H, Varavipour M. Simulation of nitrogen uptake and distribution under furrows and ridges during the maize growth period using hydrus-2D. Irrigation Science, 2019; 37(4): 495–509.

[18] Douglas L A, Bremner J M. Extraction and colorimetric determination of urea in soils. Soil Science Society of America Journal, 1970; 34(6): 859–862.

[19] Nie W B, Ma X Y, Fei L J. Evaluation of infiltration models and variability of soil infiltration properties at multiple scales: variability of soil infiltration properties. Irrigation and Drainage, 2017; 66(4): 589–599.

[20] Crevoisier D, Popova Z, Mailhol J C, Ruelle P. Assessment and simulation of water and nitrogen transfer under furrow irrigation. Agricultural Water Management, 2008; 95(4): 354–366.

[21] Liu L, Niu W Q, Guan Y H, Wu Z G, Ayantobo O O. Effects of urea

fertigation on emitter clogging in drip irrigation system with muddy water. Journal of Irrigation and Drainage Engineering, 2019; 145(9): 04019020.

[22] Šimůnek J, van Genuchten M Th, Šejna M. Development and applications of the HYDRUS and STANMOD software ackages, and related codes. Vadose Zone J, 2008; 7(2): 587–600.

[23] van Genuchten M Th. A closed-form equation for predicting the hydraulic conductivity of unsaturated soils. Soil Science Society of America Journal, 1980; 44(5): 892–898.

[24] Siyal A A, Bristow K L, Šimůnek J. Minimizing nitrogen leaching from furrow irrigation through novel fertilizer placement and soil surface management strategies. Agricultural Water Management, 2012; 115: 242–251.

[25] Kandelous M, Šimůnek J, Genuchten M, Malek K. Soil water content distributions between two emitters of a subsurface drip irrigation system. Soil Science Society of America Journal, 2011; 75(2): 488–497.

[26] Hosseiny H. Implementation of heuristic search algorithms in the calibration of a river hydraulic model. Environmental Modelling & Software, 2022; 157: 105537.

[27] Liu Z H, Cai L, Dong Q G, Zhao X L, Han J Q. Effects of microplastics on water infiltration in agricultural soil on the loess plateau, china. Agricultural Water Management, 2022; 271: 107818.

[28] Rosseel Y. Lavaan: An R package for structural equation modeling. Journal of Statistical Software, 2012; 48: 1–36.

[29] Fan Y, Chen J Q, Shirkey G, John R, Wu R, Park H, Shao C L. Applications of structural equation modeling (SEM) in ecological research: an updated review. Ecological Processes, 2016; 5(1): 238–249.

[30] Kumar S, Hari Prasad K S, Bundela D S. Effect of sodicity on soil–water retention and hydraulic properties. Journal of Irrigation and Drainage Engineering, 2020; 146(5): 04020004.

[31] Shafeeq P M, Aggarwal P, Krishnan P, Rai V, Pramanik P, Das T K. Modeling the temporal distribution of water, ammonium-n, and nitrate-n in the root zone of wheat using hydrus-2D under conservation agriculture. Environmental Science and Pollution Research, 2020; 27(2): 2197–2216.

[32] Ismail S M. Water use efficiency and bird pepper production as affected by deficit irrigation practice. International Journal of Agriculture and Forestry, 2012; 2(5): 262–267.

[33] Wang D, Liu C, Yang Y S, Liu P, Hu W, Song H Q, et al. Clipping decreases plant cover, litter mass, and water infiltration rate in soil across six plant community sites in a semiarid grassland. Science of The Total Environment, 2023; 861(2): 160692.

[34] Mailhol J C, Crevoisier D, Triki K. Impact of water application conditions on nitrogen leaching under furrow irrigation: experimental and modelling approaches. Agricultural Water Management, 2007; 87(3): 275–284.

[35] Brunetti G, Šimůnek J, Bautista E. A hybrid finite volume-finite element model for the numerical analysis of furrow irrigation and fertigation. Computers and Electronics in Agriculture, 2018; 150: 312–327.

[36] Abbasi F, Simunek J, Van Genuchten M Th, Feyen J, Adamsen F J, Hunsaker D J, Strelkoff T S, Shouse P. Overland water flow and solute transport: model development and field-data analysis. Journal of Irrigation and Drainage Engineering, 2003; 129(2): 71–81.

[37] Gärdenäs A I, Hopmans J W, Hanson B R, Šimůnek J. Two-dimensional modeling of nitrate leaching for various fertigation scenarios under micro-irrigation. Agricultural Water Management, 2005; 74(3): 219–242.

[38] Li J S, Zhang J J, Rao M J. Wetting patterns and nitrogen distributions as affected by fertigation strategies from a surface point source. Agricultural Water Management, 2004; 67(2): 89–104.